NURETH14-445

INFLUENCE OF NUMERICAL TOOLS ON THE FLOW AND HEAT TRANSFER OF SUPERCRITICAL WATER

A. Shams, D.C. Visser and F. Roelofs

Nuclear Research and Consultancy Group (NRG), Petten, The Netherlands shams@nrg.eu

Abstract

In a Supercritical Water Reactor (SCWR) the reactor core is cooled with supercritical water (SCW). For the design and operation of a SCWR, the characteristics of the heat transfer from the fuel rods to the SCW coolant needs to be well understood. These heat transfer characteristics are complex and cannot be captured by the correlations that are currently available in literature. Predicting the heat transfer to SCW has also become a challenge for Computational Fluid Dynamics (CFD) models. In the present study, the influence of numerical tools on the supercritical water flowing through a heated tube configuration has been investigated in preparation for analyses of a rod bundle validation case. A wide range of 2D axi-symmetrical and full 3D calculations are performed and compared for the SCW tube experiments of Yamagata and Ornatskiy. In addition, different meshing techniques, i.e. hybrid (hexa- and polyhedral), were used to achieve an optimal mesh resolution for such high Prandtl number flows. Furthermore, the influence of the applied meshing strategy in the transition from near wall to bulk region has been investigated for the prediction of the overall flow topology and heat transfer.

1. Introduction

Supercritical Water Reactors (SCWR) are under consideration as one of the 4th generation nuclear reactors. A SCWR is cooled with supercritical water (SCW) which has distinct advantages over subcritical water used in Light Water Reactors. First of all, SCW is a single phase fluid and, therefore, the risk of boiling crises is avoided. Furthermore, these types of reactors are expected to have high plant efficiencies because of the elevated temperatures that can be applied. The simple plant lay-out makes this type of reactors also economically attractive (see [1]). Figure 1 shows a schematic lay-out of a SCWR. In order to design the core of a SCWR, the heat transfer characteristics of the supercritical water coolant need to be better understood. The current empirical correlations for heat transfer are not suitable to describe the heat transfer to SCW across the pseudo-critical line. Furthermore, the deterioration of heat transfer results in a local, sharp increase of the temperature of the cladding. This phenomenon needs to be avoided in order to assure the integrity of the cladding.

The physical properties of water near the pseudo-critical point vary strongly. Figure 2 shows the physical properties of water at a pressure of 24.52 MPa, obtained from Lemmon et al. [2]. Near the pseudo-critical point (approximately 383 °C), small changes in temperature will result in large changes in the fluid properties. Near the pseudo-critical line the density decreases dramatically. Furthermore, there exists a large peak of thermal expansion coefficient which behaves very

similar to the specific heat. Thermal conductivity decreases with increasing temperature. It shows, however, a local maximum near the pseudo-critical point. Beyond the pseudo-critical temperature thermal conductivity decreases sharply. Similar behaviour is also shown for the dynamic viscosity. Due to the sharp increase in specific heat, there exists a large peak in the Prandtl number at the pseudo-critical point. This leads to a strong variation in the heat transfer coefficient.

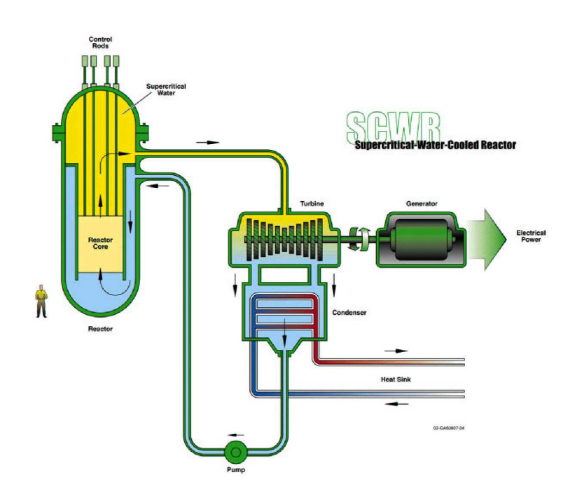


Figure 1 A schematic lay-out of a SCWR

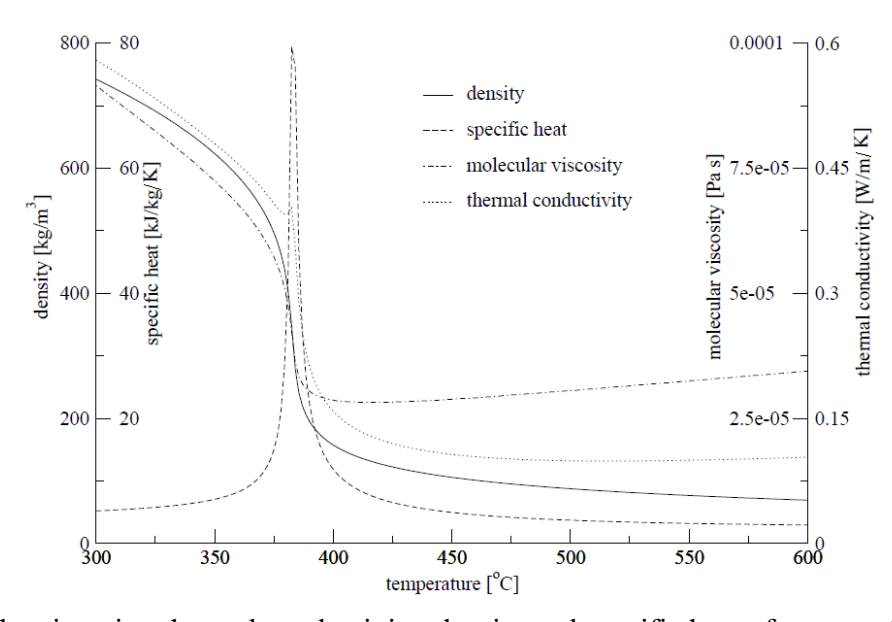


Figure 2 The viscosity, thermal conductivity, density and specific heat of water at 24.52 MPa as a function of temperature near the pseudo-critical temperature [2].

Taking into account the Dittus-Boelter equation, Nu= 0.023 Re^{0.8} Prⁿ, where n is 0.4 for heating of the fluid, and 0.3 for cooling of the fluid. It has been shown in open literature by many authors that the real heat transfer coefficient for supercritical fluids deviates from the Dittus-Boelter equation, especially near the pseudo-critical line. At relatively low heat fluxes, the heat transfer

coefficient is higher than the values predicted by Dittus-Boelter. This phenomenon is called heat transfer *enhancement*. At high heat fluxes, the heat transfer coefficient is lower than predicted by Dittus-Boelter. This phenomenon is called *heat transfer deterioration* (HTD) and can result in a local, sharp increase in the wall temperature. The design of the European SCWR design, labeled High Performance Light Water Reactor (HPLWR), requires (i) a better understanding of these characteristic heat transfer phenomena and (ii) prediction methods for heat transfer at HPLWR conditions [3]. Hence, computational fluid dynamics (CFD) and newly developed challenging numerical methods and/or models within it allow investigating the heat transfer of supercritical fluids in different geometric configurations.

Cheng et al. [3] argue that the main difficulties in the numerical analysis of supercritical fluids are related to the turbulence modelling. Due to a large variation in the thermal-physical properties, especially near the pseudo-critical point, a strong buoyancy effect and acceleration effect exist near the heated wall. A wide range of turbulence Reynolds Averaged Navier Stoked (RANS) models has been tested in [4] - [9] in order to assess their prediction capabilities for super-critical fluids. Based on these previous studies, it has been found that RANS models can successfully describe normal heat transfer of supercritical fluids. However, an important inconsistency in these turbulence models has been reported for cases with deteriorated heat transfer. This problem challenges the turbulence experts/code developers and encourages them to overcome such issues.

The present paper focuses on the numerical calculation of SCW flowing upward through a heated tube configuration in preparation for analyses of a rod bundle validation case. Sections 2, 3 and 4 of this paper give a description of the flow configuration, its parameters and the numerical strategies that have been adopted to perform the calculations, respectively. Several 2D axisymmetrical and full 3D analyses are performed and compared for the SCW tube experiments of Yamagata [10] and Ornatskiy [11]. The influence of near wall meshing and its sensitivity on the solution is given in section 5.1, followed by a detailed discussion on the influence of RANS models on the heat transfer prediction for SCW in section 5.2. In section 5.3, the applicability of a hybrid meshing techniques, using hexa- and poly-hedral cells, for the prediction of the heat transfer is investigated. Finally, based on these results some conclusive remarks and future outlooks are given.

2. Flow Geometry

In the present study, a simplified pipe case geometry has been considered by following the experimental study of Yamagata [10] and Ornatskiy [11]. Figure 3 shows the modelled geometry of the aforementioned experiments. These two experimental studies are reproduced by varying the pipe diameter accordingly, *i.e.* D=7.5 mm for Yamagata [10] and D=3.0 mm for Ornatskiy [11] cases.

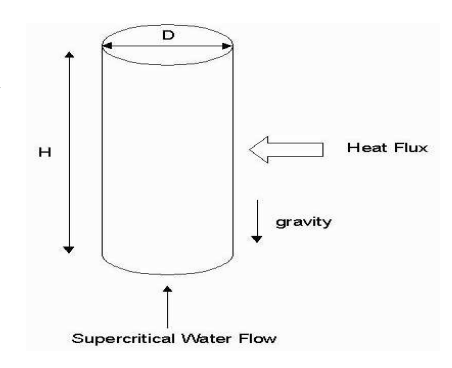


Figure 3 Schematic representation of threedimensional geometric configuration

3. Flow Parameters

In the present study, numerical calculations are performed in order to simulate the thermal hydraulic experiments of Yamagata and Ornatskiy of SCW flowing through a heated pipe. The Yamagata [10] experiments at a mass flux of 1260 kg/m²/s and a pressure of 24.52 MPa are considered at two different heat flux values, at 233 & 698 kW/m². The Ornatskiy [11] experiments at a pressure of 25.5 MPa and mass flux of 1500 kg/m²/s are considered at two different heat fluxes as well, at 1320 and 1810 kW/m². In the analyses, SCW is modelled as an incompressible, single-phase fluid under steady, isobaric, turbulent flow conditions. The temperature dependent properties of SCW are implemented in the applied CFD code Fluent for viscosity, density, thermal conductivity and specific heat. These temperature dependent properties are adopted from the NIST database [2].

4. Numerical Methods and Turbulence Modelling

The computations have been performed using the widely used commercial CFD code Fluent 6.3, described in Fluent Inc. [12]. The main fluid dynamics model describes a single phase, steady state, isobaric, turbulent flow. Hence, incompressible steady state calculations are performed by using a Reynolds Averaged Navier-Stokes (RANS) type modelling approach. In this context two different type of linear turbulence models which belong to the families of k-ε and k-ω are considered here. Detailed discussion regarding these two models and related issues will be given in section 5.2. Furthermore, second order upwind schemes have been used for spatial discretization, for details see [12].

5. Results and Discussion

Correct numerical analysis and/or prediction of SCW is directly and indirectly related to several numerical parameters. Numerous studies have highlighted that special care is required to model the thermal hydraulics of SCW. First of all, strong buoyancy and acceleration effects can take place near the heated wall due to the large variation in fluid density at the pseudo-critical point. On top of that, the large variation of thermal-physical properties at the pseudo-critical point can lead to a high Prandtl number flow regime, meaning that the thermal boundary layer is thinner than the momentum boundary layer. These typical characteristics of SCW poses a challenge for the existing turbulence models and opens the direction for new model development and/or modification of the existing ones.

Since the thermal boundary layer is thinner than the momentum boundary layer in high Prandtl number flows, special care is required to generate a fine mesh near the wall. Obviously, the extension of such a fine mesh to the complex three-dimensional geometries will be computationally very costly. On the one hand, an often applied hexahedral mesh which is not fine enough may lead to misleading results; on the other hand, the use of unstructured meshing strategies (e.g. tetrahedral or polyhedral) could be helpful. However, till now no study has been performed which can provide guidelines for the application of such meshes for supercritical fluids. In the following sections, the aforementioned three issues (near wall meshing and grid sensitivity (1), turbulence modelling (2), and three dimensional meshing techniques (3)) regarding the numerical prediction of supercritical water will be discussed.

5.1 Near Wall Meshing and Grid Sensitivity

In the present study, both 2D axi-symmetric and 3D configurations are used. In the present section, discussion regarding 2D meshing issues is given, whereas discussion regarding 3D meshing which is primarily extension in the azimuthal direction is given later in section 5.3. Nonuniform two dimensional quadrilateral meshes are employed for the 2D axi-symmetric configuration. Because of the high Prandtl number of the flow, the thermal boundary layer is much thinner than the momentum boundary layer. Therefore the mesh refinement near the wall is determined to be such that the non-dimensional distance to the wall y⁺ is approximately or less than 0.2. Therefore, the influence of the near wall mesh refinement on the accuracy of the computed results is analysed by comparing the results of meshes with different values of the nondimensional distance to the wall (y⁺). Among them the first one (i.e. Mesh A) contains 70, 000 grid points. This includes 70 points in the radial direction and 1000 grid points in the axial direction. Mesh A has an aspect ratio of around 5000 near the wall and 5 near the pipe axis. Apparently, this mesh configuration results in a high aspect ratio near the wall region and its influence on the overall flow topology needs to be checked. Hence, another mesh, i.e. Mesh B, was generated of around 546,000 grid points and has relatively small aspect ratio. Similar to the mesh A configuration, this mesh B contains 70 grid points in the radial directions with a slight modification and around 7800 points in the axial direction. This results in an aspect ratio of 1200 near the wall and around 6 near the axis region. Simulations are performed for both aforementioned experimental cases of Yamagata and Ornatskiy by using mesh A & B.

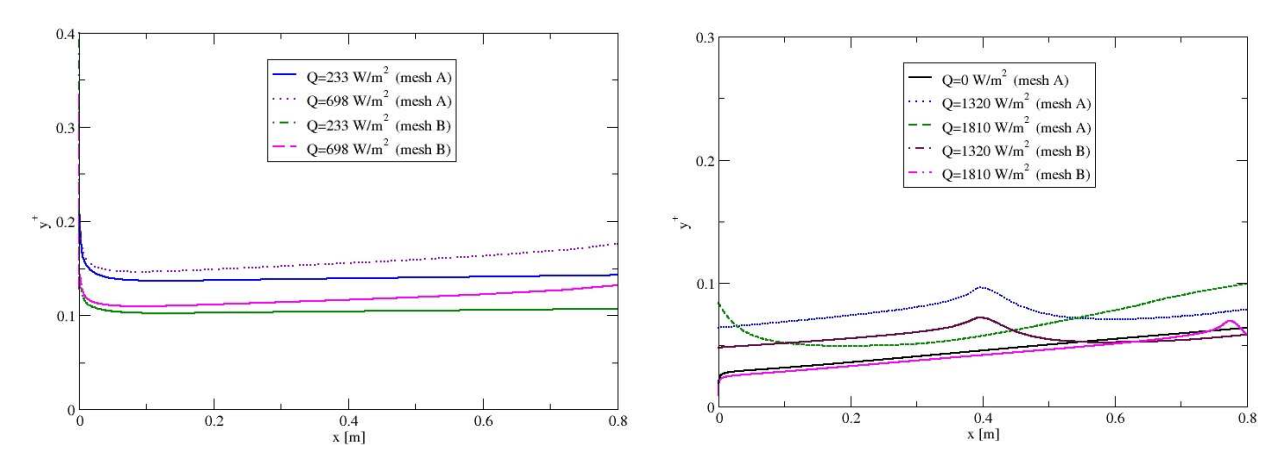


Figure 4 Evolution of y⁺ along the pipe wall for (Left) Yamagata [10] and (Right) Ornatskiy [11] configurations.

Figure 4, displays the evolution of y^+ along the wall for the considered cases. This figure demonstrates that the y^+ value remains in between 0.1 & 0.2 for both the considered Yamagata cases. A similar kind of behavior has been observed for the Ornatskiy case, where the value of y^+ is even less than 0.1 for both meshes. In spite of the fact that these meshes seem quite fine, their sensitivity needs to be checked in terms of wall temperature prediction. Figure 5, shows the comparison of predicted wall temperature for both meshes (A & B) in comparison with the experiments. One can clearly notice that there is no significant deviation in the results predicted by these meshes. This suggests that both meshes are fine enough to capture overall flow physics and prefers mesh A over B in order to reduce the computational cost.

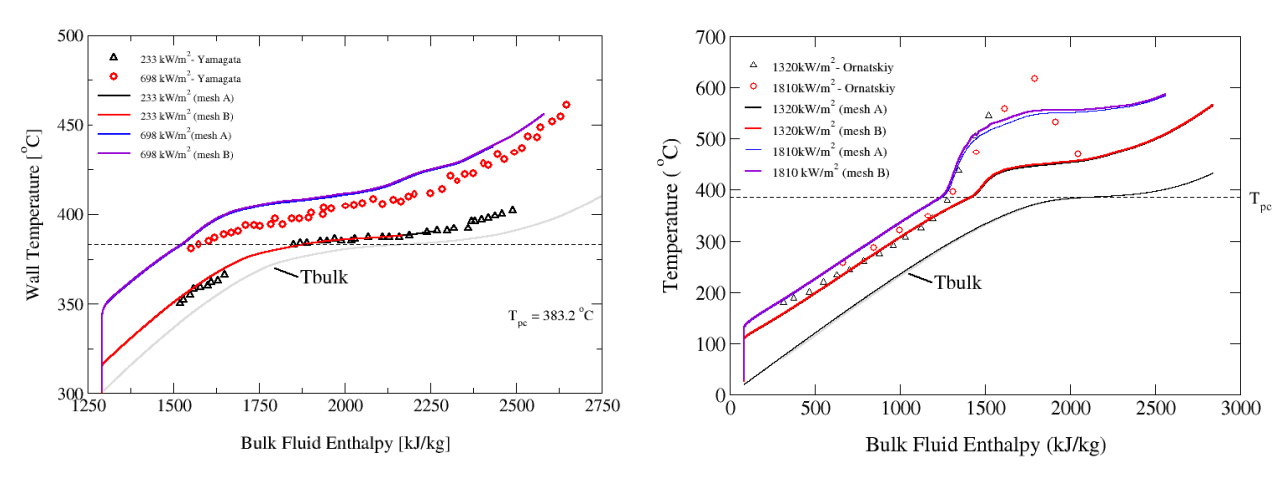


Figure 5 Evolution of wall temperature versus bulk enthalpy for the Yamagata [10] (left) and the Ornatskiy [11] (right) configuration, showing the influence of near wall meshing.

5.2 Influence of Turbulence Modelling

The Yamagata and Ornatskiy cases are considered as single phase, steady state, isobaric, turbulent flows. The physical properties of water near the pseudo-critical point vary strongly and pose difficulties for the existing turbulence models. Two different RANS turbulence models are considered in the present study, the RNG k- ϵ turbulence model with enhanced wall treatment (EWT) and the shear-stress transport (SST) k- ω turbulence model. These models are designed to give an accurate description of the flow in the near-wall region. Both models are used in previous numerical studies on wall-to-fluid heat transfer under super critical conditions. Kim et al. [4] found, in an assessment of 14 turbulence models, that the RNG k- ϵ turbulence model gave the best predictions. Palko and Anglart [6] found that the SST k- ω turbulence model performed best, in particular to predict HTD.

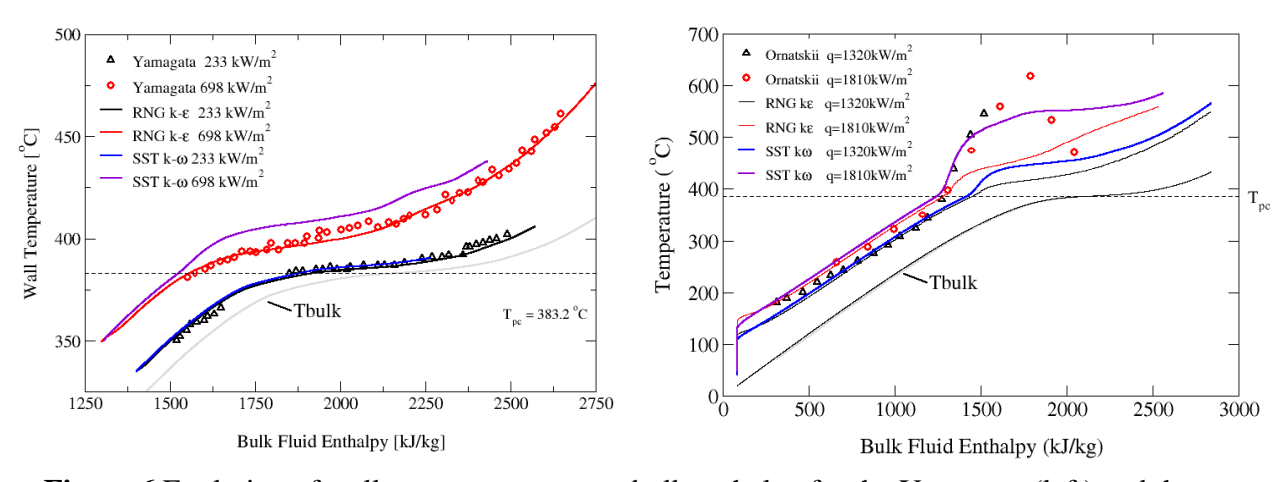


Figure 6 Evolution of wall temperature versus bulk enthalpy for the Yamagata (left) and the Ornatskiy (right) configuration, showing the influence of different turbulence models.

Figure 6 presents the numerical results obtained for Yamagata and Ornatskiy counter-parts at two different heat flux values by using mesh A. Evolution of wall temperature along with the bulk enthalpy is compared for the aforementioned RANS models. Let us first consider the computed

cases of Yamagata, in which there is no heat transfer deterioration. At low heat flux value, i.e. 233 kW/m^2 , both models shows similar type of results and close to the experiments. At high heat flux, i.e. 698 kW/m^2 , RNG k- ϵ models show a close agreement to the experimental results, however, SST k- ω does not seem to reproduce the correct wall temperature profile. For the Ornatskiy experiment, the obtained results display surprising behavior. The RNG k- ϵ model does not predict the HTD observed in the experiment. Although not exactly matching the HTD found experimentally, the SST k- ω model clearly predicts HTD. Furthermore, this HTD reproduced by SST k- ω for relatively low heat flux case is not much enhanced in comparison to the experiments and shows the inconsistency of existing RANS models. Such behaviour of the RANS models needs to be further studied for different type of scenarios.

5.3 Three-Dimensional Configuration / Meshing and Related Issues

As mentioned earlier, the focus of this paper is on the numerics of heat transfer to SCW in preparation for the analyses of a rod bundle validation case. It has been demonstrated [6]-[7] that a fine mesh is required near the heated walls to capture the complex heat transfer phenomena to SCW. The application of such a refined mesh to complex three-dimensional geometries will be computationally very costly. A hybrid meshing technique with hexahedral cells near the wall and polyhedral cells in the bulk can help to control the number of cells in such 3D cases. In order to assess the hybrid meshing technique for heat transfer to SCW, two 3D hybrid meshes (mesh C and mesh D) have been generated and tested for the Yamagata and Ornatskiy experiments. The effect of the meshing strategy is observed by comparing the experimental results and the 2D axisymmetrical results presented in the previous sections. Special focus is on the influence of the transition from the hexahedral cells near the wall to the polyhedral cells in the bulk region.

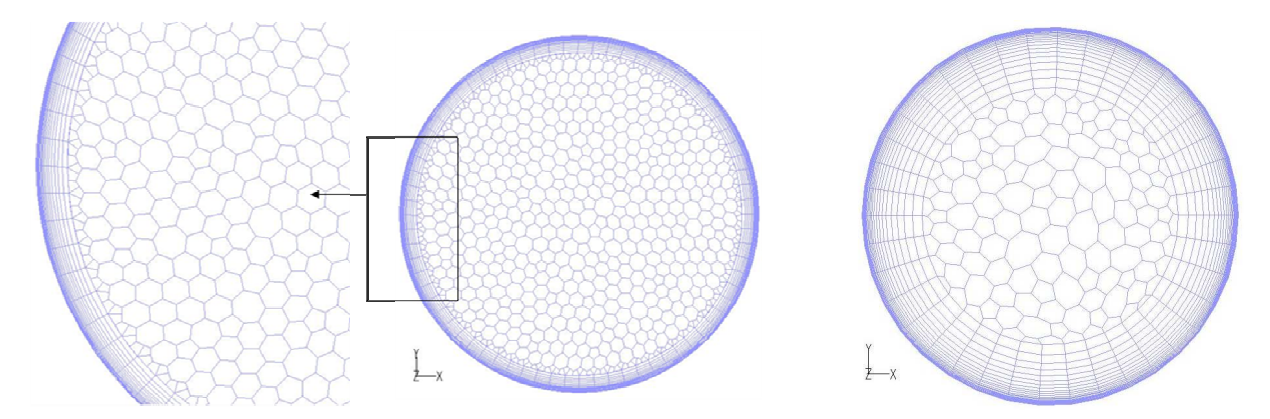


Figure 7 Cross-sections of the 3D hybrid mesh C (left) and mesh D (right). Mesh C is generated in Gambit and contains hanging nodes. Mesh D is generated in STAR- CCM+.

Figure 7 illustrates the 3D hybrid mesh C and mesh D. Mesh C contains around 4.6 M grid points and mesh D around 3.6 M cells. Both meshes consist of a structured hexahedral mesh near the wall similar to that of the 2D axi-symmetrical mesh A and a polyhedral mesh in the centre core region. Mesh C was originally generated in Gambit as a combination of hexa- and tetrahedral cells, and then the tetrahedral cells were converted into polyhedral cells within the environment of Fluent. As a result of this mesh conversion in Fluent, hanging nodes are created at the

transition between the hexahedral near wall cells and the polyhedral bulk cells (see the inset in Figure 7).

In order to check out the influence of the so-called hanging nodes on the numerical solution, simulations are performed for the Yamagata case. Before going into details the evolution of axial and radial profiles of temperature along the 3D pipe are shown and compared in Figure 8. As expected, there is no appearance of flow three-dimensionality. More importantly, a slight bump in the radial temperature profile has been observed near the wall region. This bump corresponds to the radial location where these hanging nodes appear. This is more clearly noticeable in Figure 9, which shows the radial profile of the axial velocity halfway the heated pipe.

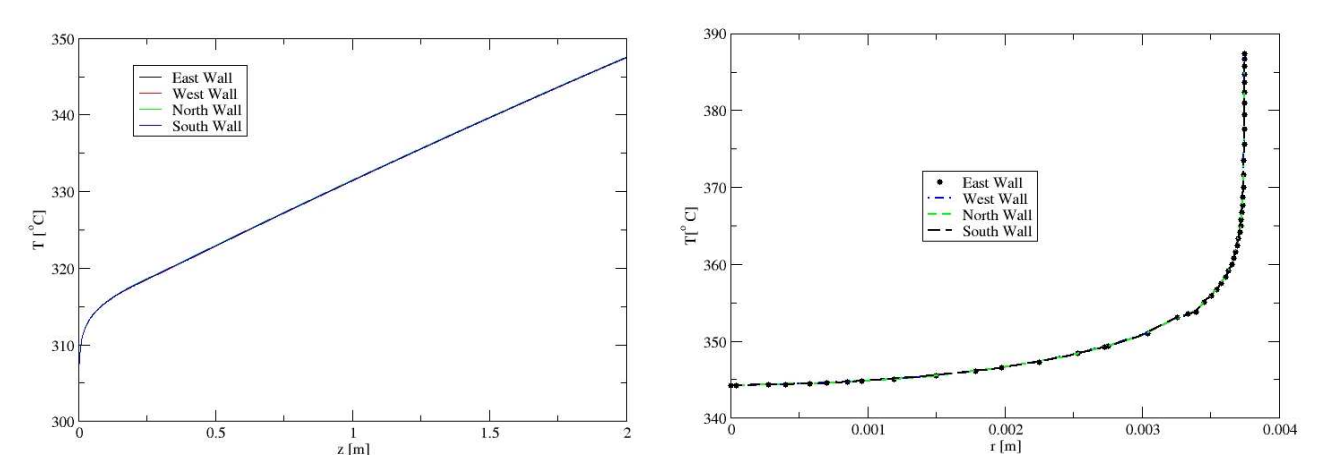


Figure 8 Temperature profile along the pipe wall in axial direction (left) and in radial direction at z = 1m (right).

Although the considered flow configuration is axi-symmetric and does not contain any swirl flow, this transition in the mesh near the wall may lead to unphysical behavior. Hence, it was decided to extend the prism layer of the hexahedral mesh outside the high gradient flow region. Consequently, the hybrid mesh obtained from Gambit/Fluent leads to a high number of mesh cells, as it does not provide enough control during the conversion of the mesh in Fluent. Therefore, a new mesh was generated in STAR-CCM+ [13], which provided a better control on the polyhedral mesh in the centre core region. The resulting mesh (mesh D) is shown in Figure 7 on the right side. The velocity profile obtained with mesh D is compared with the previous results in Figure 9. One can clearly notice that there appear no bumps in the velocity profile obtained by using mesh D. This is simply because the hexa- to polyhedral transition is shifted to a low gradient flow region.

As shown in Figure 7, hanging nodes are avoided in the hybrid mesh generated with STAR-CCM+. In order to test the effect of hanging nodes on the numerical solution, a mesh similar to mesh C was reproduce in STAR CCM+ without hanging nodes. This mesh C from STAR CCM+ is shown in Figure 10. Again, simulations were performed with this 3D hybrid mesh and a comparison is given in Figure 11. A zoom near the mesh transition region is also shown and one can notice that the bump in velocity profile also appears in the mesh without hanging nodes. However, this bump is not much pronounced in comparison with hanging node case. The results

suggest that one should be careful while generating the computational mesh, especially sudden jumps in the cell size near mesh transition regions should be avoided.

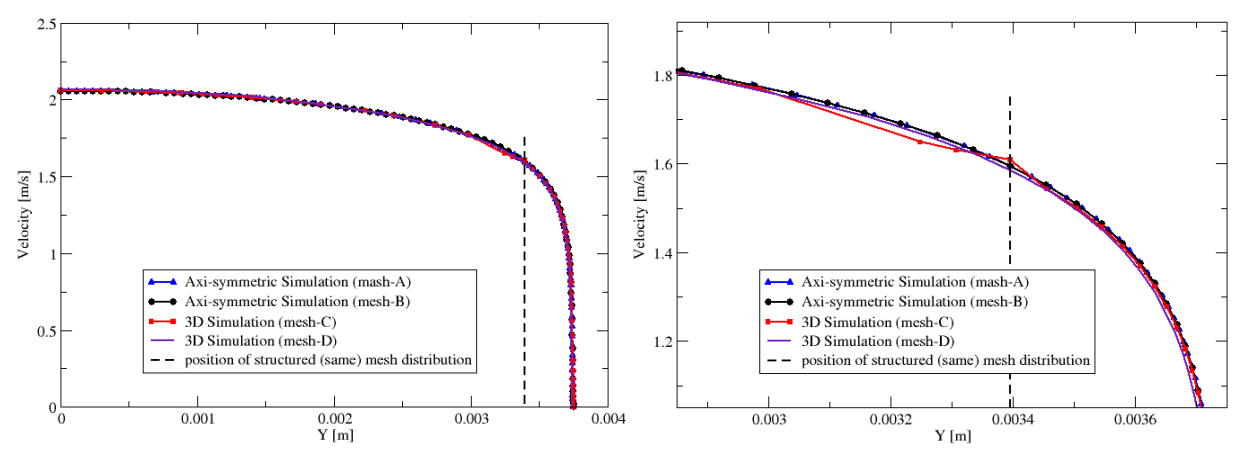


Figure 9 Radial profile of the axial velocity at z = 1m. On the left the velocity profile over the full radius and on the right a close-up of this profile near the wall.

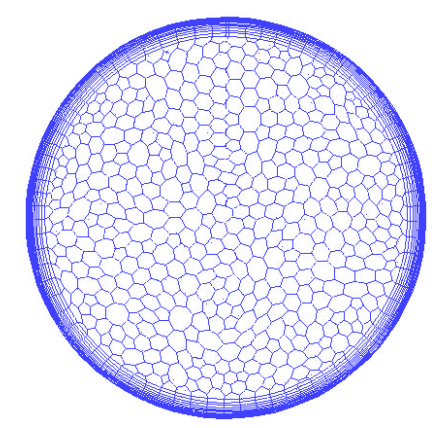


Figure 10 Cross-section of 3D hybrid mesh C without hanging nodes as generated in STAR-CCM+.

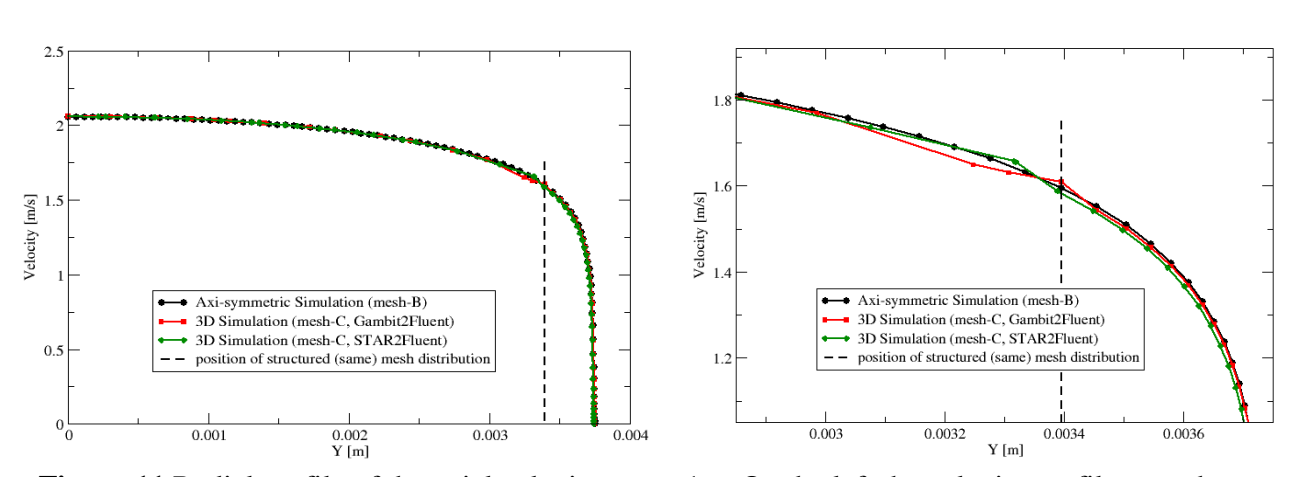


Figure 11 Radial profile of the axial velocity at z = 1m. On the left the velocity profile over the full radius and on the right a close-up of this profile near the wall.

Moreover, the influence of these meshes has also been investigated for the overall heat transfer. These calculations are performed by using SST k-ω models and results are shown in Figure 12. Evolution of wall temperature against the bulk enthalpy obtained by using these 3D meshes is compared for two different heat flux cases of Yamagata and Ornatskiy. One can depict from Figure 12 that all 2D axi-symmetric and 3D meshes result in a similar heat transfer behavior and its respective deterioration. This was to be expected because of the axi-symmetric behavior of the flow configuration. Nevertheless, it validates the use of hybrid meshes for heat transfer analyses with SCW, which allows application of this meshing technique for more complex 3D geometries like e.g. a wire wrap rod bundle, avoiding redundant mesh requirements for RANS type calculations. At the same time, one should be careful with sudden jumps in the cell size which can introduce numerical errors in the flow.

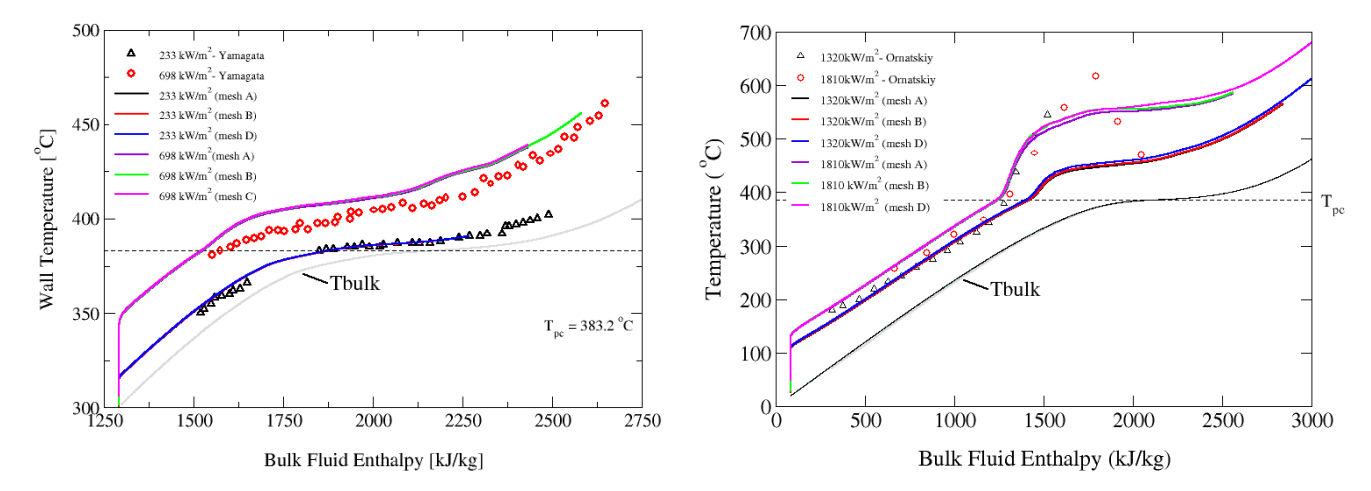


Figure 12 Evolution of wall temperature versus bulk enthalpy for the Yamagata (left) and the Ornatskiy (right) configuration, showing the influence of 3D meshes

6. Conclusive Remarks and Future Outlooks

In the present study, the influence of numerical tools on the prediction of supercritical water flowing through a heated tube configuration has been investigated in preparation for analyses of a rod bundle validation case. For this purpose a wide range of 2D axi-symmetrical and full 3D calculations are performed and compared for the SCW tube experiments of Yamagata and Ornatskiy. Several aspects of CFD tools were investigated to check their influence on the flow and heat transfer prediction of super-critical water.

Comparison of meshes on an axi-symmetric configuration was made by varying the y^+ value and mesh aspect ratio in an acceptable range. The obtained results indicated no significant influence on overall flow topology by varying the y^+ value of first near wall mesh in the range of 0.1-0.2. A similar behavior was also observed by varying the cells aspect ratio, which somehow seems obvious because of the axi-symmetric behavior of flow regime. However, this parameter is of vital importance while dealing with complex geometry containing highly three-dimensional and/or swirl flow configurations.

Furthermore, the influence of meshing was further tested for different 3D meshing techniques, i.e. hybrid (hexa- and polyhedral), which were used to achieve an optimal mesh resolution for such high Prandtl number flows. Although no significant difference in the overall heat transfer and HTD was noticeable, however, the sudden jump in mesh cells that appears near in the transition (of hexa- and polyhedral) lead to erroneous results. Hence, one needs to be careful while generating such type of computational meshes. Moreover, this mesh transition was shifted to a region of low gradient flow and works well. However, this may lead to redundantly high mesh resolution for RANS type calculations. Thanks to the versatile meshing capability of STAR-CCM+ this high mesh numbers was also reduced by having a good control on unstructured mesh in the centre core region.

Despite of the various past studies related to the validation of RANS models for super-critical flow regimes; still correct prediction of these flows has been an issue and offers big challenges for turbulence model developers. A large variation in the thermal-physical properties, especially near the pseudo-critical point, causes a strong buoyancy effect and acceleration effect exists near the heated wall. In addition, due to the sharp increase in specific heat capacity, there exists a large peak of the Prandtl number at the pseudo-critical point. This lead to a strong variation in heat transfer coefficient. Two recommended RANS models, i.e. RNG k-ε and SST k-ω, were tested and compared with experimental data of Yamagata and Ornatskiy. For simple heat transfer cases, RNG k-E shows good agreement with the experiments. However, this very model fails to reproduce the HTD effect for high heat flux cases. On the other hand, SST k-ω displays the signatures of predicting this HTD for high heat flux values, not so much pronounced for relatively low flux case. Surprisingly, this SST k-ω shows bigger discrepancy compared to the experimental values than RNG k-epsilon model for the investigated cases. Such type of inconsistency in prediction by the models, pose difficulties in the selection of turbulence models and in gaining trust on the obtained numerical solution. Hence, this opens the direction in the realm of turbulence modelling, either to modify the existing models or suggest the newer ones, which should be able to deal with strong buoyancy effects, large variation of Prandtl number and HTD type scenarios.

7. Acknowledgements

The work described in this paper was funded by the Dutch Ministry of Economic Affairs.

8. References

- [1] U.S. Department of Energy, 2002, Nuclear Energy Research Advisory Committee, Generation IV International Forum, "A Technology Roadmap for the Generation IV Nuclear Energy Systems," GIF-002-00, http://gif.inel.gov/roadmap/pdfs/gen_iv_roadmap.pdf.
- [2] E. W. Lemmon, M. O. McLinden and D. G. Friend, 2005, "Thermophysical Properties of Fluid Systems", NIST Chemistry WebBook, NIST Standard Reference Database Number 69, P.J. Linstrom and W.G. Mallard, National Institute of Standards and Technology, Gaithersburg MD.
- [3] X. Cheng, T. Schulenberg, 2001, Heat Transfer at Supercritical Pressures Literature Review and Application to an HPLWR, *Scientific* Report, FZKA6609, Forschungszentrum Karlsruhe, Germany.

- [4] S.H. Kim, Y.I. Kim, Y.Y. Bae, B.H. Cho, 2004, "Numerical Simulation of the Vertical Upward Flow of Water in a Heated Tube at Supercritical Pressure", Proc. Of ICAPP 2004, Paper 4047, Pittsburgh, USA.
- [5] X. Chang and E. Laurien, 2005, "CFD Analysis of Heat Transfer in Supercritical Water in Different Flow Channels", Proc. of GLOBAL 2005, Paper 369, Tsukuba, Japan.
- [6] D. Palko and H. Anglart, 2007, "Theoretical and Numerical Study of Heat Transfer Deterioration in HPLWR", Proc. of the Int. Conference NENE, Paper 205, Portorož, Slovenia.
- [7] F. Roelofs, J. A. Lycklama à Nijeholt, E. M. J. Komen, M. Löwenberg and J. Starflinger, 2007, "CFD Validation of a Supercritical Water Flow for SCWR Design Heat and Mass Fluxes", Proc. of ICAPP 2007, Paper 7043, Nice, France.
- [8] D.C. Visser, J.A. Lycklama a Nijeholt and F. Roelofs, 2008, "CFD Predictions of Heat Transfer in Super Critical Flow Regime, Proc. of ICAPP 2008, Paper 8155, Anaheim USA.
- [9] L. Chandra, J.A. Lycklama a Nijeholt, D.C. Visser and F. Roelofs, 2009, "CFD analyses on the influence of wire wrap on the heat transport in supercritical fluid," Proc. of NURETH-13, Paper 1014, Kanazawa, Japan.
- [10] K. Yamagata, K. Nishikawa, S. Hasegawa, T. Fuji and S. Yoshida, 1972, "Forced Convective Heat Transfer to Supercritical Water Flowing in Tubes", Int. J. Heat and Mass Transfer, vol. 15, pp. 2575-2593.
- [11] A.P. Ornatskiy, L.F. Glushchenko, S.I. Kalachev, 1971, "Heat transfer with rising and falling flows of water in tubes of small diameter at supercritical pressures", Therm. Eng., 18 (5), 137.
- [12] Fluent Inc., 2006, FLUENT 6.3 User's Guide.
- [13] STAR-CCM+, 2010, User Manual, Version 5.06.007. CD Adapco, London.